Article

Not peer-reviewed version

TPI and GAPDH Interact with Rad9, Linking Glycolytic Enzymes to Cancer

Vivienne X.Y. Chua †, Joyce M.X. Yip †, Melody T.K. Cho, Sumi Z.Q. Lin, Rich Tan, Donna G.K. Lee, Kexin Dai, Teck K. Lim, Quingsong Lin, Rachel Lehming-Teo, Ophry Pines, Norbert Lehming *

Posted Date: 2 May 2026

doi: 10.20944/preprints202604.2181.v1

Keywords: RAD9; TPI1; GAPDH; DNA Damage Response

 doi:10.20944/preprints202604.2181.v1

Article

TPI and GAPDH Interact with Rad9, Linking Glycolytic Enzymes to Cancer

Vivienne X.Y. Chua [1,†], Joyce M.X. Yip [1,†], Melody T.K. Cho [1], Sumi Z.Q. Lin [1], Rich Tan [1], Donna G.K. Lee [1], Kexin Dai [1], Teck K. Lim [2], Qingsong Lin [2], Rachel Lehming-Teo [1], Ophry Pines [3] and Norbert Lehming [1,*]

[1] Department of Microbiology & Immunology and Cancer Programme at NUSMED, Yong Loo Lin School of Medicine, National University of Singapore, Singapore

[2] Department of Biological Sciences, Faculty of Science, National University of Singapore, Singapore

[3] Department of Microbiology and Molecular Genetics, IMRIC, Faculty of Medicine, Hebrew University of Jerusalem, Israel

* Correspondence: micln@nus.edu.sg; Tel.: +65-6516-3499

† These authors contributed equally to this work.

Abstract

Cancer cells, like yeast, use fermentation despite the presence of oxygen, a phenomenon called aerobic glycolysis. The advantage is that it maintains most of the C-C bonds of glucose, allowing highly proliferating cells to produce the biomolecules that are necessary for cytokinesis. However, aerobic glycolysis is less energy-efficient than respiration, and it must operate at a higher frequency and produces more toxic by-products like methylglyoxal, which damages DNA. Cancer cells, like yeast cells, developed efficient systems to repair their damaged DNA. This makes cancer cells resistant to radiotherapy, which requires a combination with chemotherapy using drugs that inhibit DNA repair. However, this converts healthy cells to cancer cells, indicating that more research is required regarding the relationship between glycolysis and cancer. Using yeast as a model, we have discovered that the glycolytic enzymes TPI1 and GAPDH interact with the DNA damage-dependent checkpoint Rad9p. Furthermore, we have isolated TPI1 and GAPDH mutant strains that are unable to repair their damaged DNA. The TPI1 mutant strain has lower TPI enzymatic activity, suggesting that it accumulates methylglyoxal, while the GAPDH mutant strains have normal GAPDH enzymatic activity, confirming that GAPDH moonlights in the DNA Damage Response.

Keywords: RAD9; TPI1; GAPDH; DNA Damage Response

1. Introduction

"There is no Cure for this Disease." - Hilaire Belloc (Belloc, 1907).

"Tumours destroy man in a unique and appalling way, as flesh of his own flesh which has somehow been rendered proliferative, rampant, predatory and ungovernable. They are the most concrete and formidable of human maladies, yet despite more than 70 years of experimental study they remain the least understood." - Francis Peyton Rous, tumour virologist, Nobel Lecture, 1966.

Cancer is the principal cause of lethality worldwide, accounting for nearly 10 million deaths in 2020, or nearly one in six deaths (WHO, 2023; Ferlay, 2020). Deregulated cellular metabolism is a hallmark of cancer that characterizes the cancer cell's adjustments of energy metabolism for it to grow and divide (Hanahan, 2011). In the presence of oxygen, normal human cells inhibit fermentation and process glucose to pyruvate via glycolysis in the much more energy-efficient mitochondrial oxidative phosphorylation, known as the Pasteur Effect (Moulin, 2023; Weinberg, 2014). An interesting observation that cancer cells carry out aerobic glycolysis was reported by Warburg in the 1920s, who also coined the term. In the presence of oxygen, the Warburg Effect, or aerobic glycolysis occurs, converting glucose to lactate in the presence of oxygen (Pecorino, 2012). A similar phenomenon

 doi:10.20944/preprints202604.2181.v1

occurs in yeast, where it is known as the Crabtree Effect (Crabtree, 1929). In alcohol-producing yeast cells, aerobic glycolysis is triggered within a few seconds (Crabtree, 1929), while in tumour cells, the Warburg Effect requires protein expression and takes days to develop (Martins Pinto, 2023). Aerobic glycolysis allows yeast and human cancer cells to generate energy in the form of ATP and NADH, while maintaining C-C bonds that proliferating cells require for the synthesis of biomolecules (Vander Heiden, 2009). However, per molecule of glucose, respiration produces approximately 40 – 2 = 38 ATP molecules, while aerobic glycolysis produces only 4 – 2 = 2 ATP molecules. Therefore, aerobic glycolysis consumes much more glucose than respiration. We decided to use the budding yeast *Saccharomyces cerevisiae* as a model system to study the link between metabolism and cancer, as both yeast and human cancer cells are highly proliferative and rely on aerobic glycolysis to generate energy while maintaining C-C bonds to produce biomolecules like deoxyribose that are required to duplicate the DNA before cell division.

There are many known links between glycolysis and DNA damage. Methylglyoxal (MG) is a toxic by-product of glycolysis that damages DNA (Iacobini, 2023; Richard 1991), and cells relying on aerobic glycolysis have efficient DNA repair systems, making cancer cells resistant to radiotherapy (Groelly, 2023). Chemotherapy with drugs that inhibit DNA repair promotes the killing of cancer cells on one hand but causes tumorigenesis of healthy cells on the other hand, as the failure to repair damaged DNA is even another hallmark of cancer (Hanahan, 2011). MG is a potent and emerging biological factor involved in the onset and progression of cancer (Bellahcene, 2018). MG is a strong glycation agent in the body and leads to alterations of proteins and DNA and cellular dysfunction (Bellier, 2019). Triosephosphate Isomerase (TPI) catalyzes the interconversion of dihydroxyacetone phosphate (DHAP) and glyceraldehyde-3-phosphate (GAP) in the glycolysis pathway (Colasanti, 2009). Glyceraldehyde 3-phosphate dehydrogenase (GAPDH) is the next glycolytic enzyme which catalyzes the conversion of GAP into glycerate-1,3-bisphosphate (Nicolescu, 2023; Supplementary Figure S1). TPI (Supplementary Figure S8) is highly expressed in many types of human tumors and is involved in the migration and invasion of cancer cells (Chen, 2017). GAPDH (Supplementary Figure S11) plays a role in several cancer-related biological processes and was reported to be commonly dysregulated in multiple cancer types (Wang, 2023). Many metabolic enzymes such as hexokinase and phosphoglycerate kinase 1 are known to function in tumour development (Lu, 2018). Hexokinase in the first step of glycolysis is known to enter the nucleus and interact with nuclear proteins in acute myeloid leukaemia (AML) (Thomas, 2022). GAPDH was shown to facilitates homologous recombination repair by stabilizing RAD51 in an HDAC1-dependent manner (Shi et al., 2023). Upon DSB occurrence, GAPDH translocates into the nucleus and is involved in homologous recombination repair by stabilizing RAD51. According to the model proposed by Shi and co-workers, the interaction with GAPDH disassociates HDAC1 from its inhibitor Maspin.

Rad9p, an adaptor protein that triggers the DNA Damage Response (DDR), is required for cell cycle checkpoint function (Kiely et al., 2026). By mediating phosphorylation of important effector kinases like Rad53p and Chk1p, Rad9p facilitates the amplification of initial signals in response to DNA damage (Toh, 2003). Because of the ability of Rad9p to associate with double-stranded breaks, it is speculated that Rad9p also initiates these checkpoint signal transduction cascades by acting as a DNA damage sensor (Naiki, 2004). Rad9p is required throughout the cell cycle as it has been shown to function at G1/S, intra-S, and G2/M (Siede, 1993; Paulovich, 1997; Weinert, 1988). Rad9p is phosphorylated during normal progression of the cell cycle but becomes hyperphosphorylated by Mec1p and Tel1p in response to DNA damage (Vialard, 1998; Emili, 1998). Activated Rad9p then stimulates Mec1p phosphorylation of the effector kinases Chk1p and Rad53p (Blankley, 2004; Ma, 2006; Sweeney, 2005). Chk1p and Rad53p phosphorylation leads to various processes associated with cellular arrest, such as transcriptional upregulation of DNA damage repair genes, transcriptional repression of cyclins, and stabilization of replication forks (Chen, 2004; Weinert, 1998). Rad9p has two BRCT (BRCA1) domains that facilitate Rad9p-Rad9p interaction after DNA damage (Soulier, 1999). It also has a tandem Tudor domain that binds to double-stranded DNA (Lancelot, 2007). *rad9* gene deletion mutants are viable but exhibit sensitivity to X-ray and UV irradiation, fail to arrest in

 doi:10.20944/preprints202604.2181.v1

response to DNA damage, and are prone to chromosomal instability (Weinert, 1988; Weinert, 1990; Fasullo, 1998). No single human ortholog has been identified; instead, in humans there exists a family of proteins, which includes BRCA1 and 53BP1, that contain tandem BRCT domains (Alpha-Bazin, 2005; Bork, 1997).

Hypothesis

Aerobic glycolysis, which proliferating cells use, is much less energy-efficient than respiration. Therefore, glycolysis linked to fermentation (to alcohol in yeast cells and to lactic acid in human cancer cells) operates at a much higher frequency than glycolysis linked to the TCA cycle in respiration. The toxic glycolytic by-product MG damages DNA, and yeast and human cancer cells had to develop efficient systems to repair their damaged DNA thus. We hypothesize that, in addition to sensing dsDNA breaks, Rad9p could senses the quantity and activity status of metabolic enzymes. According to this model, high levels and activity of glycolytic enzymes would signal to Rad9p that the DNA-damaging agent MG is being produced.

2. Materials and Methods

2.1. PCR-Based Random Mutagenesis of GAPDH

For each tube, 1µL of template was added. 49µL of mix containing 10µL 5X buffer, 3µL 25mM Magnesium Sulfate, 1µL nucleotides, 2µL forward primer, 2µL reverse primer, 30µL water and 1µL *Taq* enzyme was distributed to each tube. The tubes were then mixed and spun down for 7000 rpm for 10 seconds. Finally, they were placed in the PCR machine with the programme indicated below.

Step 1: 95.0°C 0:01:00
Step 2: 95.0°C 0:00:30
Step 3: 45.0°C 0:00:30
Step 4: 72.0°C 0:01:00; 34 x return to step 2
Step 5: 72.0°C 0:10:00
Step 6: 4.0°C ∞

2.2. Mass Spectrometry

GST fusion proteins were purified with gluthathione beads subjected to SDS PAGE. The gel was stained with InstantBlue Coomassie Protein Stain. The bands of the protein of interest were cut out and in-gel trypsinated. The tryptic peptides were subjected to liquid chromatography – mass spectrometry (LC-MS) analysis using an Eksigent nanolC Ultra and ChiPLC-nanoflex (Eksigent) in trap-elute configuration, with a 200 µm × 0.5 mm trap column and a 75 µm × 150 mm analytical column. Both trap and analytical columns were made of ChromXP C18-CL, 3 µm (Eksigent). Peptides were separated by a gradient formed by 2% ACN, 0.1% FA (mobile phase A) and 98% ACN, 0.1% FA (mobile phase B): 5% to 7% of mobile phase B in 0.1 min, 7% to 30% of mobile phase B in 10 min, 30% to 60% of mobile phase B in 4min, 60% to 90% of mobile phase B in 1 min, 90% to 90% of mobile phase B in 5 min, 90% to 5% of mobile phase B in 1 min and 5% to 5% of mobile phase B in 10 min, at a flow rate of 300 nl/min. The MS analysis was performed on a TripleTOF 5600 system (AB SCIEX, Foster City, CA, USA) in Information Dependent Mode. MS spectra were acquired across the mass range of 400–1250 m/z in high resolution mode (>30000) using 250 ms accumulation time per spectrum. A maximum of 10 precursors per cycle were chosen for fragmentation from each MS spectrum with 100 ms minimum accumulation time for each precursor and dynamic exclusion for 8 s. Tandem mass spectra were recorded in high sensitivity mode (resolution >15000) with rolling collision energy on.

 doi:10.20944/preprints202604.2181.v1

Peptide identification and the detection of post-translational modifications were carried out with the ProteinPilot 5.0.3.0 software Revision 5313 (AB SCIEX) using the Paragon database search algorithm (5.0.3.0.5312), against a protein sequence database (6128 entries) of the yeast *Saccharomyces cerevisiae*.

2.3. Generation of the Yeast Strain Expressing Human HsTPI1 in Place of Endogenous Tpi1p

The tryptophane auxotrophic *BY4741/2/3ΔW* strains have been described (Wang et al., 2020). *BY4141ΔW* and *BY4742ΔW* cells were transformed with the *URA3*-marked single-copy plasmid PactT316-Tpi1, which expresses Tpi1p under the control of the strong constitutive *ACT1* promoter/terminator cassette. Next, the *TPI1* gene was replaced with the *HIS3* gene by homologous recombination and the strains were mated to generate the diploid *BY4743ΔW TPI1::HIS3+PactT316-Tpi1* strain, which was transformed with *LEU2*-marked single- and multi-copy plasmids expressing Nub-HA-Tpi1p wild-type and mutant or Nub-HA-HsTPI1 wild-type and mutant under the control of the strong constitutive *ADH1* promoter/terminator cassette or the empty vector control. Plasmid shuffle was performed on FOA plates (Figure 3).

2.4. Generation of the Yeast Strain Expressing Gapdh Mutants in Place of Endogenous GAPDH

The *TDH1* gene of *BY4741ΔW* and BY4742ΔW was replaced with the *TRP1* gene. Next, the *TRP1* marker was recovered with the help of the *TR-hisG-URA3-hisG-P1* cassette of NKY1009 (Alani et al., 1987) and the *URA3* marker was recovered on an FOA plate. Subsequently, the *TDH2* gene was replaced with the *LEU2* gene and the *BY4741ΔW* strain was transformed with PactT316-Tdh2, while the BY4742ΔW strain was transformed with PactT316-Tdh3 for no apparent reason. Finally, the *TDH3* gene was replaced with *HIS3* and the strains were mated to generate *BY4743ΔW TDH1::hisG/TDH1::hisG; TDH2::LEU2/TDH2::LEU2; TDH3::HIS3/TDH3::HIS3+PactT316-Tdh2+PactT316-Tdh3*, named *BY4743ΔWΔTDH1-3+PactT316-Tdh23* in this study. The strain was transformed with the *TRP1*-marked plasmids PactT424-GST-Tdh123 wild-type and mutants and PactT316-Tdh23 was shuffled out on an FOA plate.

2.5. Yeast Breaking for Enzyme Assay

Cells were resuspended and transferred into a screw cap tube before 100µL of appropriate buffer (KDalert buffer for GAPDH assay, yeast lysis buffer for TPI assay) was added. Afterwards, glass beads of equal volume to the cells were added into the same screw cap tube. Next, the cells were broken in the bead beater at 6000 rpm, 3x20s, 10 seconds interval. After each cycle, the tubes were placed onto an ice box for 3 minutes, the breaking and cooling were repeated 3 times. Subsequently, the cells were placed into a 4°C centrifuge and spun down at 15000 rpm for 10 minutes. Finally, the supernatant was transferred into a new eppendorf tube.

2.6. GAPDH Enzyme Assay

BY4743 yeast cells were inoculated in 10ml YPDA culture media and grown overnight to OD 1 to 2. Afterwhich, cells were lysed and total protein concentration was measured using nanodrop. The KDalert™ GAPDH Assay Kit by invitrogen was used to measure GAPDH enzyme activity. To a cuvette, 88.8µL of solution A, 0.68µL of solution B and 0.47µL of solution C was added. Solutions A, B and C contain the required substrates: glyceraldehyde-3-phosphate (G-3-P), phosphate ions and NAD^+ to measure GAPDH enzyme activity. 20µL of yeast protein extract was added and mixed with 900µL of water in the cuvette. After that, the cuvette was placed into the spectrophotometer to measure GAPDH enzyme activity at 615nm for 5 minutes in 30 second intervals. The results of the measurement were then recorded.

2.7. TPI Enzyme Assay

BY4743 cells were inoculated overnight in 25ml YPDA culture media to OD 1 to 2. Afterwhich, cells were lysed and total protein concentration measured using nanodrop. To a cuvette, 44µL of TPI

 doi:10.20944/preprints202604.2181.v1

Assay Buffer, 2µL of TPI Enzyme Mix, 2µL of TPI Developer and 2µL of TPI Substrate was added. On top of that, a volume of extract from yeast breaking depending on the protein concentration measured in the nanodrop was added. The cuvette was then topped up to 100µL with TPI Assay Buffer. 900µL of sterile water was added to the cuvette and mixed. After that, the cuvette was placed into the spectrophotometer to measure TPI enzyme activity at 450nm for 5 minutes in 30 seconds intervals. The results of the measurement were then recorded.

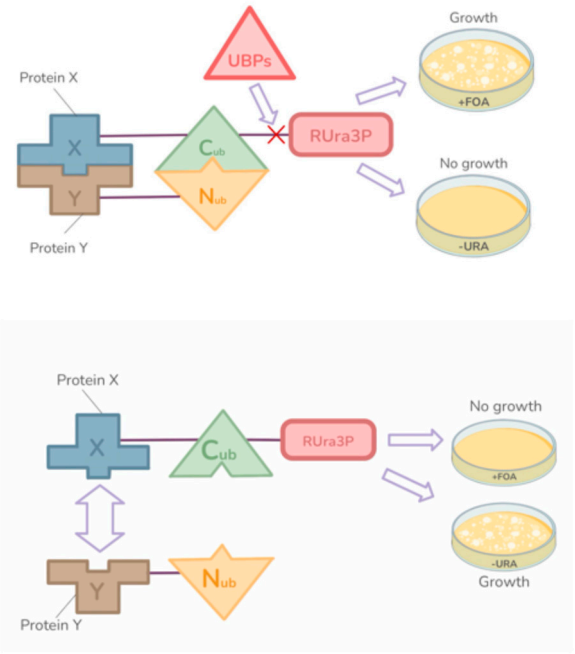

Figure 1. The Split-Ub Assay. The Nub construct consists of a protein of interest fused to the N-terminal half of ubiquitin. While the Cub construct is made of a protein of interest fused to the C-terminal of ubiquitin extended by the RUra3 protein, which is OMP whose first amino acid had been replaced with an arginine (R). *Left Panel:* **Presence of Protein-Protein interaction:** If the two proteins of interest (Protein X and Y) interact inside the living cell, the Cub attached to Protein Y will be in close proximity with the Nub that was fused to protein X. This results in the formation of a native-like Ubiquitin moiety that will be recognised by ubiquitin-specific proteases (UBPs), leading to UBPs cleaving the bond between Cub and RUra3p. Free RUra3p will be rapidly degraded by 26S proteasomes due to the N-end rule. As a result, there will no longer be Ura3p in the cells. When these cells are plated on a fluoroorotic acid plate (+FOA), Ura3p is not present to convert FOA into toxic fluorouracil, allowing for the cells to survive. However, when these cells are plated onto plates lacking uracil (-URA), there will not be Ura3p present to synthesise uracil required for RNA synthesis, thereby resulting in no cell growth. *Right Panel:* **Absence of Protein-Protein interaction:** If the two proteins of interest (Protein X and Y) do not interact inside the living cell, the Cub that is attached to Protein X and the Nub fused to protein Y will not be in close proximity. As such, a full native-like ubiquitin moiety will not be formed and the UBPs will not cleave the peptide bond between the Cub and RUra3p. As a result, RUra3p will not be degraded and will still be present inside the yeast cell. When these cells are plated onto FOA plates (+FOA), Ura3p will be present to convert FOA into toxic fluorouracil, resulting in the cells to die. On the other hand, when these cells are plated onto plates lacking uracil (-URA), the cells will be able to make uracil, allowing for the cells to grow.

3. Results and Discussion

We tested the yeast DNA damage-dependent checkpoint Rad9p for interaction with yeast metabolic enzymes in the Split-Ub assay. Figure 2 shows that Rad9p interacted with GAPDH (Tdh1p, Tdh2p & Tdh3p, lines 1, 2, 5, 6, 7, 8), Fumarate Reductase (Frd1p, lines 11, 12), Hexokinase 2 (Hxk2p, lines 13, 14), Phosphoglucokinase (Pgk1p, lines 17, 18), cytosolic Malate Dehydrogenase 2 (Mdh2p, lines 23, 24), Phosphofructokinase 1 (Pfk1p, lines 25, 26) and Triosephosphate Isomerase (Tpi1p, lines

 doi:10.20944/preprints202604.2181.v1

31, 32). When the cells were grown under conditions of DNA damage (+ HU), all these interactions became stronger and Rad9p interacted additionally with Glucokinase 1 (Glk1p, lines 35, 36). No interaction was observed for Malic Enzyme (Mae1p, lines 19, 20) nor for the mitochondrial dicarboxylate carrier Dic1p (lines 29, 30).

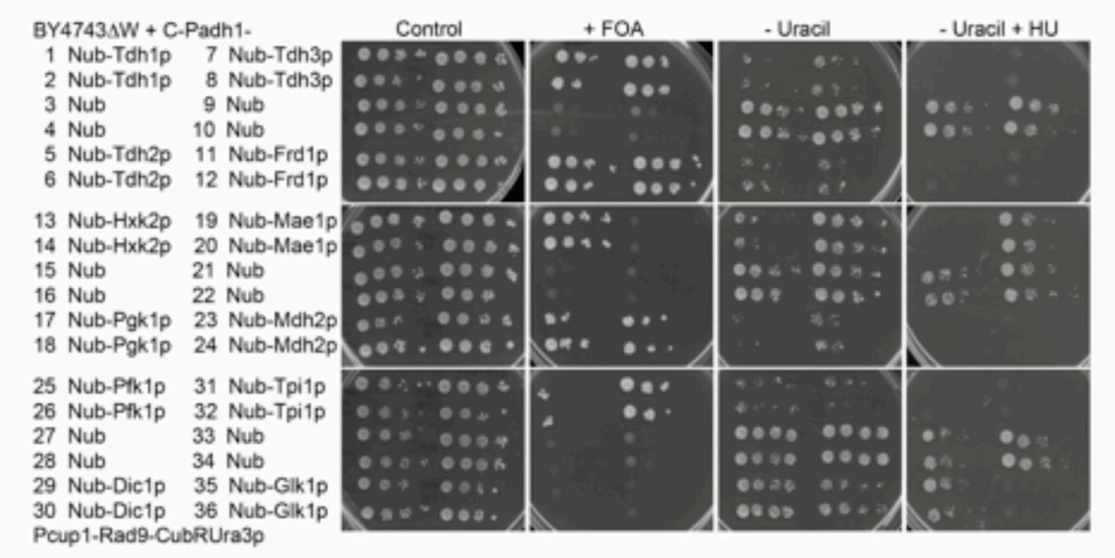

Figure 2. Rad9p interacted with metabolic enzymes in living yeast cells. Tenfold serial dilutions of cells expressing the indicated proteins were spotted onto the depicted plates and incubated at 28°C for six days. Protein-protein interaction inside the living cells is revealed by growth on the FOA plates and by lack of growth on the plates lacking uracil.

The glycolytic enzymes Tpi1p, which interconverts DHAP and GAP and generates the DNA damaging agent MG as a by-product, and GAPDH, which converts DHAP to 1,3BPG, were chosen for further study. Human patients suffering from Triosephosphate isomerase deficiency (TPID) express the HsTPI1E105D mutant protein (Daar, 1986). TPID is an autosomal recessive multisystem disorder characterized by congenital hemolytic anemia, progressive neuromuscular dysfunction, susceptibility to bacterial infection, and cardiomyopathy (uniprot/P60174). While the patients have lower TPI1 enzymatic activity in the serum, the mutation reduces the stability of TPI1 and does not alter its enzymatic activity. In order to determine if the E105D mutation or the more severe E105A mutation would affect the DDR in yeast, we expressed Nub fusions of human HsTPI1 and its mutant derivatives under the control of the strong *ADH1* promoter from single-copy (C) and multi-copy (D) plasmids in yeast cells lacking the essential chromosomal *TPI1* gene that were kept alive with the help of the *URA3*-marked plasmid PactT316-Tpi1, expressing Tpi1p from the *ACT1* promoter. The left panels of Figure 3 shows that human HsTPI1 and its mutant derivatives were able to complement the yeast gene deletion strain and grow on the FOA plate, which counter-selects the PactT316-Tpi1p plasmid (lines 1 to 12), with cells expressing the HsTPI1E105A mutant protein from the single-copy vector displaying a growth phenotype (line 9). The figure further shows that the HsTPI1E105A mutant strain was sensitive to the DNA-damaging agent HU (lines 17, 18). Western Blots were performed to compare the expression levels of HsTPI1 with its mutant derivatives. The right panels of Figure 3 show that the E105A mutant protein was expressed at even higher levels than wild-type HsTPI1.

 doi:10.20944/preprints202604.2181.v1

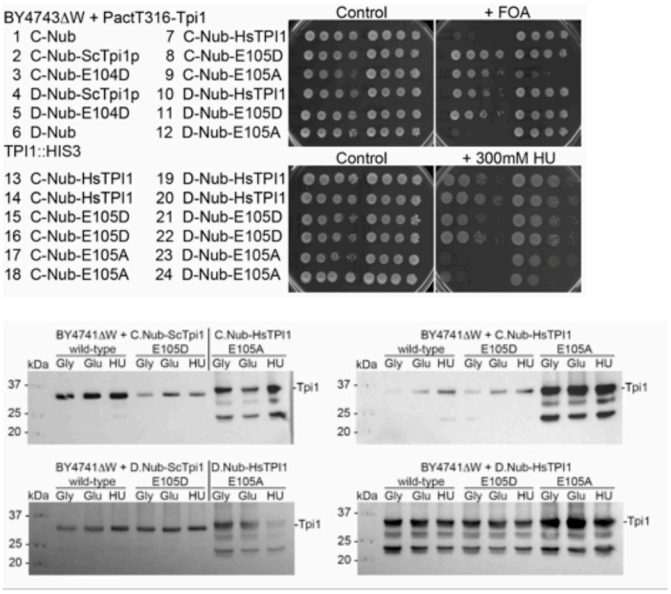

Figure 3. Yeast cells expressing human HsTPI1E105A in place of endogenous Tpi1p are viable but unable to repair their damaged DNA. *Left Panels:* The URA3-marked plasmid PactT316-Tpi1 expressing endogenous Tpi1p was removed on the FOA plate (right top panel), and cells expressing Nub-HsTPI1 from single-copy (C) and multi-copy (D) plasmids were tenfold serially diluted and spotted onto HU plates to test for their ability to repair their damaged DNA. *Right Panels:* HsTPI1E105A is expressed at higher protein levels than wild-type HsTPI1. Yeast cells were grown to mid-log phase in glucose liquid media (Glu) and incubated for two hours with 300mM HU (HU). Cells were boiled in SDS loading dye, separated by SDS PAGE and visualized with an anti-HA antibody.

In order to determine if the E105A mutation reduced the enzymatic activity of HsTPI1, TPI commercial enzyme assays (Abcam) were performed with extracts from yeast cells expressing HA-tagged HsTPI1 and its mutant derivative in place of yeast Tpi1p. Figure 4 shows that the E105A mutation reduced the enzymatic activity of HsTPI1 two-fold. The figure further shows that exposure to DNA damaging conditions for two hours reduced the enzymatic activity of HsTPI1 two-fold as well. One possible explanation of the HU sensitivity of the E105A mutant strain is that the defective TPI1E105A enzyme results in the accumulation of DHAP, which dephosphorylates to the DNA-damaging agent MG. Supplementary Figure S8 shows the location of E105 relative to the catalytically active residues H96 and E166.

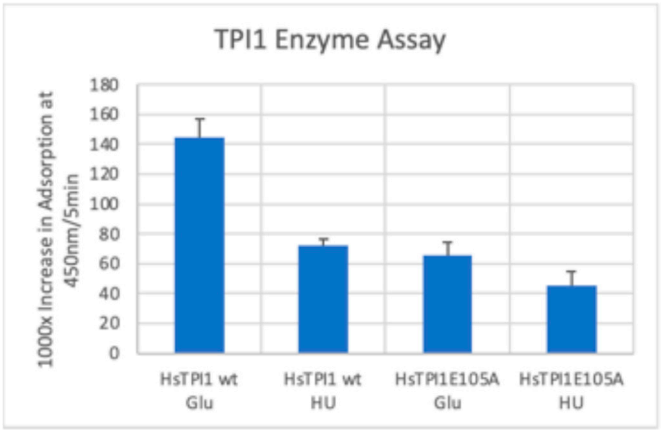

Figure 4. The E105A mutation reduced the enzymatic activity of HsTPI1 twofold. Yeast cells expressing HsTPI1 and the E105A derivative in place of yeast Tpi1p were grown to mid-log phase in glucose liquid media (Glu) and incubated with 300mM HU for two hours (HU). Extracts were generated with bead beating and the protein concentration was determined by nanodrop. 80 µg of extract were used for the TPI1 assay and the increase in

 doi:10.20944/preprints202604.2181.v1

adsorption at 450 nm was measured for 5 minutes. The error bars represent the standard deviation between triplicates. The student T-test was 0.000415057 for wt Glu vs E105A Glu and 0.000355559 for wt Glu vs wt HU.

Enzyme activity could be modulated by post-translational modification, and we purified GST-Tpi1p from yeast cells that had been grown under normal conditions and from yeast cells that had been incubated with HU for two hours. Mass spectrometry revealed that Tpi1p was specifically modified at 30 residues upon exposure to conditions of DNA damage (Figure 5). Our results for the TPI1 assay indicate that these modifications reduce the enzymatic activity of Tpi1p.

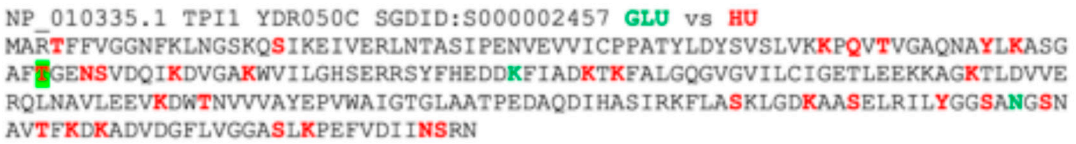

Figure 5. Tpi1p is post-translationally modified at 30 residues under conditions of DNA damage. Residues shown in bold red were found to be modified specifically when the cells were grown with HU and residues shown in bold green were found to be modified specifically when the cells were grown under normal, glucose conditions. A figure with the nature of these modifications can be found in the appendix. T75 was phosphorylated when the cells had been grown under normal conditions and ubiquitinated when the cells had been exposed to 300mM HU for two hours.

Mass Spectrometry was also carried out with GST-Tdh1p purified from yeast cells grown under normal conditions and under conditions of DNA damage. The results showed that Tdh1p was methylated at S149 and T152 when the cells had been grown under normal conditions and phosphorylated at S146 and S149 and methylated at N153 when the cells had been exposed for two hours to conditions of DNA damage (Figure 6). These residues are close to the catalytically active C150, and S149 binds GAP (uniprot), indicating that these modifications modify the enzymatic activity of Tdh1p (Supplementary Figure S11).

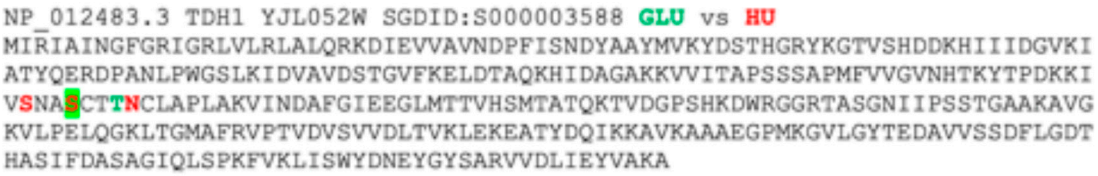

Figure 6. Tdh1p is post-translationally modified at three residues under conditions of DNA damage. Residues shown in bold red were found to be modified specifically when the cells were grown with HU and residues shown in bold green were found to be modified specifically when the cells were grown under normal, glucose conditions. A figure with the nature of these modifications can be found in the appendix. S149 was methylated when the cells had been grown under normal conditions and phosphorylated when the cells had been exposed to 300mM HU for two hours.

In order to block post-translational modifications, S146 and S149 were mutated to A and expressed in yeast as GST fusions. Figure 7 shows that these mutant proteins were rapidly degraded when the cells were exposed for two hours to conditions of DNA damage. The figure further shows that the mutant proteins failed to complement a *TDH1-3* gene deletion strain that was kept alive with the *URA3*-marked plasmids PactT316-Tdh2/3, expressing Tdh2p and Tdh3p from the *ACT1* promoter, indicating that S146 and S149 are important for the enzymatic function of the essential Tdh1p.

 doi:10.20944/preprints202604.2181.v1

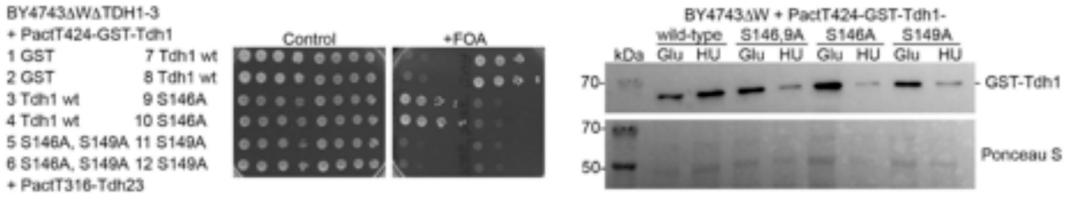

Figure 7. The Tdh1S146A and Tdh1S149A mutant proteins fail to complement a *TDH1-3* gene deletion strain. *Left panel:* Yeast cells expressing the indicated GST fusions in place of endogenous Tdh1-3 proteins were tenfold serial diluted and spotted onto plates with and without FOA. *Right panel:* Yeast cells expressing the indicated GST fusions were grown to mid-log phase in glucose liquid media (Glu) and exposed to two hours of DNA damage (HU). Cells were boiled in SDS loading dye and proteins were separated by SDS-PAGE. Proteins were blotted onto nitrocellulose and GST fusions were visualized with the help of an anti-GST antibody.

We used the *TDH1-3* gene deletion strain to generate GAPDH mutants that are sensitive to HU with the goal to study the role of GAPDH in the DDR. Random PCR-based mutagenesis coupled with gap repair and plasmid shuffle on FOA plates followed by replica plating resulted in the Tdh1p mutant proteins H60R, L88R, L103S and K192S,T244A (Figure 8) and the Tdh3p mutant protein L219S (Figure 9). Subcloning revealed that only the T244A mutation caused sensitivity to HU and that the K192S mutation had no effect.

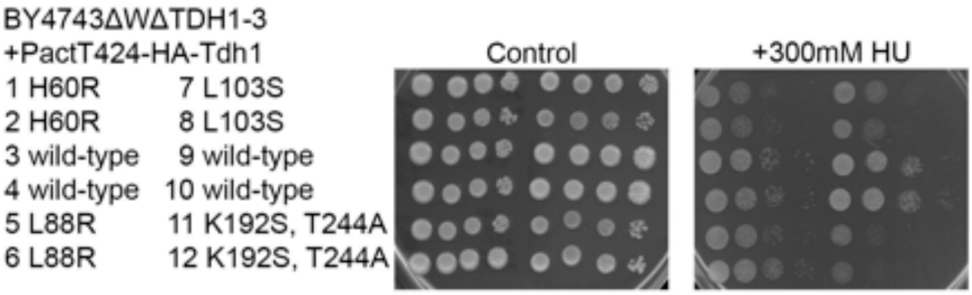

Figure 8. Random mutagenesis identified Tdh1 mutant proteins that confer sensitivity to HU. Tenfold serial dilutions of cells expressing the indicated proteins were spotted onto control plates and onto plates containing 300mM HU.

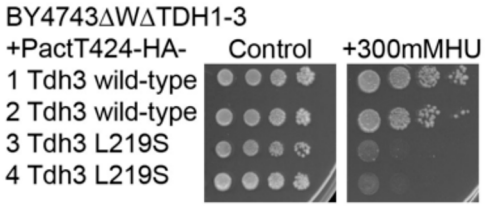

Figure 9. Random mutagenesis identified the Tdh3L219S mutant strain that is sensitive to HU. Tenfold serial dilutions of cells expressing the indicated proteins were spotted onto control plates and onto plates containing 300mM HU.

In order to determine if the mutations reduced the GAPDH enzymatic activity, GAPDH commercial enzyme assays (Invitrogen) were performed with extracts from yeast cells expressing GST-Tdh1/3p and their mutant derivatives in place of yeast Tdh1/3p. Figure 10 shows that exposure to DNA damaging conditions for two hours increased the enzymatic activity of all fusions. Surprisingly, all mutant enzymes were fully active. One possible explanation is that GAPD

 doi:10.20944/preprints202604.2181.v1

moonlights in the DDR with a function independent from its ability to interconvert GAP and 1,3BPG: by stabilizing Rad51p (Shi et al., 2023).

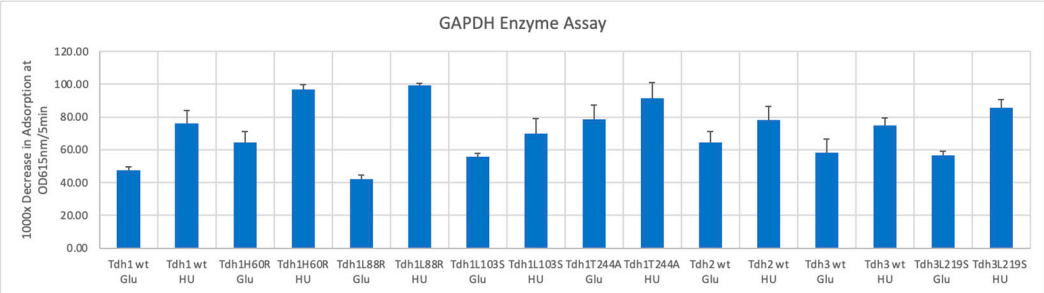

Figure 10. DNA damage conditions stimulated GAPDH activity, but the mutations had no effect on enzyme activity for GAP. Yeast cells expressing the indicated proteins were grown to mid-log phase in glucose liquid media (Glu) and treated with 300mM HU for two hours (HU). Extracts were generated with bead beating and the protein concentration was determined by nanodrop. 80 ug of extract were used for the GAPDH assay and the decrease in adsorption at 615 nm was measured for 5 minutes. The error bars represent the standard deviation between triplicates. The student T-tests were below 0.05 for all Glu vs HU pairs with the exception of the one for Tdh2 (0.10079935).

4. Conclusions

The glycolytic enzymes TPI and GAPDH were implicated in the DDR as they interacted with the DNA damage-dependent checkpoint Rad9p, and mutants that were unable to repair their damaged DNA were isolated. The TPI1E105A mutant protein showed reduced enzymatic activity, suggesting that MG levels might be high in this strain, while the GAPDH mutants were enzymatically fully active, presumably reflecting that GAPDH moonlights in the DDR by preventing proteolytic degradation of HDAC1.

Supplementary Materials: The following supporting information can be downloaded at the website of this paper posted on Preprints.org.

Author Contributions: VXYC contributed Figures 1 to 4; JMXY contributed the yeast strains *BY4743ΔW TPI1::HIS3/TPI1::HIS3+PactT316-Tpi1p* used in Figure 3 to 5 and *BY4743ΔW TDH1:hisG/TDH1:hisG TDH2::LEU2/TDH2::LEU2 TDH3::HIS3/TDH3::HIS3+PactT316-Tdh2+PactT316-Tdh3* used in Figures 6 to 10; RT purified GST-Tpi1 ± HU and contributed Figure 5; DGKL purified GST-Tdh1p ± HU and contributed Figure 6; DK contributed Figure 7, MTKC & SZQL contributed Figures 8 to 10; TKL and QL performed and analysed the MS; RLT, OP and NL designed the experiments, mentored VXYC, JMXY, MTKC, SZQL, RT, DGLK & KD, and wrote the manuscript.

Funding: This research was funded by Ministry of Education grant number A-8000724-00-00.

Institutional Review Board Statement: Not applicable.

Informed Consent Statement: Not applicable.

Data Availability Statement: The original contributions presented in this study are included in the article/supplementary material. Further inquiries can be directed to the corresponding author.

Acknowledgements: This work was supported by grant A-8000724-00-00 from the Ministry of Education (MOE) of Singapore to NL. This work was also supported by the German-Israeli Foundation (Nexus grant no. I-1561-412.13/2023) to OP. The authors would like to thank Mr Jasper Tan and Ms Leong May Lin for excellent technical help.

Conflicts of Interest: The authors declare that they have no conflicting interest.

 doi:10.20944/preprints202604.2181.v1

References

1 Alpha-Bazin B, et al. (2005) Boundaries and physical characterization of a new domain shared between mammalian 53BP1 and yeast Rad9 checkpoint proteins. Protein Sci 14(7):1827-39 PMID: 15987907

2 Bellahcene A, Nokin MJ, Castronovo V, Schalkwijk C. (2018). Methylglyoxal-derived stress: An emerging biological factor involved in the onset and progression of cancer. Maastricht, Netherlands. Retrieved from: https://www.sciencedirect.com/science/article/abs/pii/S1044579X17300871?via%3Dihub

3 Bellier J, Nokin MJ, Lardé E, Karoyan P, Peulen O, Castronovo V, Bellahène A. (2019). Methylglyoxal, a potent inducer of AGES, connects between diabetes and cancer. Paris, France. Retrieved from: https://www.sciencedirect.com/science/article/abs/pii/S0168822718316267

4 Bhardwaj A, Das S. SIRT6 deacetylates PKM2 to suppress its nuclear localization and oncogenic functions. Proc Natl Acad Sci U S A. 2016 Feb 2;113(5):E538-47. doi: 10.1073/pnas.1520045113. Epub 2016 Jan 19. PMID: 26787900; PMCID: PMC4747762.

5 Belloc, H (1907) Cautionary Tales for Children. Duckworth 3 Heinretta Street, London, W.C.

6 Blankley RT and Lydall D (2004) A domain of Rad9 specifically required for activation of Chk1 in budding yeast. J Cell Sci 117(Pt 4):601-8 PMID: 14709724

7 Bork P, et al. (1997) A superfamily of conserved domains in DNA damage-responsive cell cycle checkpoint proteins. FASEB J 11(1):68-76 PMID: 9034168

8 Chen Y and Sanchez Y (2004) Chk1 in the DNA damage response: conserved roles from yeasts to mammals. DNA Repair (Amst) 3(8-9):1025-32 PMID: 15279789

9 Chen T, Huang Z, Tian Y, Wang H, Ouyang P, Chen H, Wu L, Lin B, He R. (2017) Role of triosephosphate isomerase and downstream functional genes on gastric cancer. Oncol Rep. 38(3):1822-1832. doi: 10.3892/or.2017.5846. PMID: 28737830.

10 Colasanti T, Delunardo F, Margutti P, Vacirca D, Piro E, Siracusano A, Ortona E. (2009) Autoantibodies involved in neuropsychiatric manifestations associated with systemic lupus erythematosus. J Neuroimmunol. 212(1-2):3-9. doi: 10.1016/j.jneuroim.2009.05.003. PMID: 19500858.

11 Crabtree HG. Observations on the carbohydrate metabolism of tumours. Biochem J. 1929;23(3):536-45. doi: 10.1042/bj0230536. PMID: 16744238; PMCID: PMC1254097.

12 Daar IO, Artymiuk PJ, Phillips DC, Maquat LE. Human triose-phosphate isomerase deficiency: a single amino acid substitution results in a thermolabile enzyme. Proc Natl Acad Sci U S A. 1986 Oct;83(20):7903-7. doi: 10.1073/pnas.83.20.7903. PMID: 2876430; PMCID: PMC386831.

13 Emili A (1998) MEC1-dependent phosphorylation of Rad9p in response to DNA damage. Mol Cell 2(2):183-9 PMID: 9734355

14 Fasullo M, et al. (1998) The Saccharomyces cerevisiae RAD9 checkpoint reduces the DNA damage-associated stimulation of directed translocations. Mol Cell Biol 18(3):1190-200 PMID: 9488434

15 Ferlay J, Ervik M, Lam F, Colombet M, Mery L, Piñeros M, et al. (2020) Global Cancer Observatory: Cancer Today. Lyon: International Agency for Research on Cancer; https://gco.iarc.fr/today

16 Gao X, Wang H, Yang JJ, Liu X, Liu ZR. Pyruvate kinase M2 regulates gene transcription by acting as a protein kinase. Mol Cell. 2012 Mar 9;45(5):598-609. doi: 10.1016/j.molcel.2012.01.001. Epub 2012 Feb 2. PMID: 22306293; PMCID: PMC3299833.

17 Groelly FJ, Fawkes M, Dagg RA, Blackford AN, Tarsounas M. Targeting DNA damage response pathways in cancer. Nat Rev Cancer. 2023 Feb;23(2):78-94. doi: 10.1038/s41568-022-00535-5. Epub 2022 Dec 5. PMID: 36471053.

18 Hanahan D, Weinberg RA. Hallmarks of cancer: the next generation. (2011) Cell. 144(5):646-74. doi: 10.1016/j.cell.2011.02.013. PMID: 21376230.

19 Iacobini C, Vitale M, Pugliese G, Menini S. The "sweet" path to cancer: focus on cellular glucose metabolism. Front Oncol. 2023 May 25;13:1202093. doi: 10.3389/fonc.2023.1202093. PMID: 37305566; PMCID: PMC10248238.

20 Ismail SA, Park HW. Structural analysis of human liver glyceraldehyde-3-phosphate dehydrogenase. Acta Crystallogr D Biol 21Crystallogr. 2005 Nov;61(Pt 11):1508-13. doi: 10.1107/S0907444905026740. Epub 2005 Oct 19. PMID: 16239728.

 doi:10.20944/preprints202604.2181.v1

22 Jenkins JL, Tanner JJ. High-resolution structure of human D-glyceraldehyde-3-phosphate dehydrogenase. Acta Crystallogr D Biol Crystallogr. 2006 Mar;62(Pt 3):290-301. doi: 10.1107/S0907444905042289. Epub 2006 Feb 22. PMID: 16510976.

23 Lancelot N, et al. (2007) The checkpoint Saccharomyces cerevisiae Rad9 protein contains a tandem tudor domain that recognizes DNA. Nucleic Acids Res 35(17):5898-912 PMID: 17726056

24 Lehming, N (2002) Analysis of protein-protein proximities using the split-ubiquitin system. Brief Funct Genomic Proteomic.1:230-238. https://doi.org/10.1093/bfgp/1.3.230

25 Lu Z, Hunter T. Metabolic Kinases Moonlighting as Protein Kinases. Trends Biochem Sci. 2018 Apr;43(4):301-310. doi: 10.1016/j.tibs.2018.01.006. Epub 2018 Feb 17. PMID: 29463470; PMCID: PMC5879014.

26 Lv L, Xu YP, Zhao D, Li FL, Wang W, Sasaki N, Jiang Y, Zhou X, Li TT, Guan KL, Lei QY, Xiong Y. Mitogenic and oncogenic stimulation of K433 acetylation promotes PKM2 protein kinase activity and nuclear localization. Mol Cell. 2013 Nov 7;52(3):340-52. doi: 10.1016/j.molcel.2013.09.004. Epub 2013 Oct 10. PMID: 24120661; PMCID: PMC4183148.

27 Ma JL, et al. (2006) Activation of the checkpoint kinase Rad53 by the phosphatidyl inositol kinase-like kinase Mec1. J Biol Chem 281(7):3954-63 PMID: 16365046

28 Mande SC, Mainfroid V, Kalk KH, Goraj K, Martial JA, Hol WG. Crystal structure of recombinant human triosephosphate isomerase at 2.8 A resolution. Triosephosphate isomerase-related human genetic disorders and comparison with the trypanosomal enzyme. Protein Sci. 1994 May;3(5):810-21. doi: 10.1002/pro.5560030510. PMID: 8061610; PMCID: PMC2142725.

29 Martins Pinto M, Paumard P, Bouchez C, Ransac S, Duvezin-Caubet S, Mazat JP, Rigoulet M, Devin A. The Warburg effect and mitochondrial oxidative phosphorylation: Friends or foes? Biochim Biophys Acta Bioenerg. 2023 Jan 1;1864(1):148931. doi: 10.1016/j.bbabio.2022.148931. Epub 2022 Oct 29. PMID: 36367492.

30 Moulin AM. Pasteur et l'entrée du vin dans la modernité scientifique [Pasteur and the entry of wine into scientific modernity]. Med Sci (Paris). 2023 May;39(5):458-462. French. doi: 10.1051/medsci/2023060. Epub 2023 May 23. PMID: 37219351.

31 Naiki T, et al. (2004) Association of Rad9 with double-strand breaks through a Mec1-dependent mechanism. Mol Cell Biol 24(8):3277-85 PMID: 15060150

32 Nicolescu CM, Bumbac M, Buruleanu CL, Popescu EC, Stanescu SG, Georgescu AA, Toma SM. (2023) Biopolymers Produced by Lactic Acid Bacteria: Characterization and Food Application. Polymers (Basel). 15(6):1539. doi: 10.3390/polym15061539. PMID: 36987319; PMCID: PMC10058920.

33 NRDO, National Registry of Diseases Office (2023) Singapore Cancer Registry Annual Report 2021. https://www.nrdo.gov.sg/docs/librariesprovider3/default-document-library/scr-ar-2021-web-report.pdf?sfvrsn=591fc02c_0

34 NRDO, National Registry of Diseases Office (2021) Cancer in Singapore 2017-2021. https://www.nrdo.gov.sg/docs/librariesprovider3/default-document-library/scr-ar-2021-infographicfaa60392d61d475aaf7a7d71fc928b87.pdf?sfvrsn=51bb444f_0#:~:text=From%202017%2D2021%2C%20cancer%20was,for%2028.2%25%20of%20all%20deaths.

35 Paulovich AG, et al. (1997) RAD9, RAD17, and RAD24 are required for S phase regulation in Saccharomyces cerevisiae in response to DNA damage. Genetics 145(1):45-62 PMID: 9017389

36 Park JB, Park H, Son J, Ha SJ, Cho HS. Structural Study of Monomethyl Fumarate-Bound Human GAPDH. Mol Cells. 2019 Aug 31;42(8):597-603. doi: 10.14348/molcells.2019.0114. PMID: 31387164; PMCID: PMC6715340.

37 Pecorino L (2012) Molecular Biology of Cancer: Mechanisms, Targets, and Therapeutics. 3rd Ed. Oxford University Press.

38 Richard JP (1991) Kinetic Parameters for the Elimination Reaction Catalyzed by Triosephosphate Isomerase and an Estimation of the Reaction's Physiological Significance. Biochemistry. 30(18):4581-5. doi: 10.1021/bi00232a031. PMID: 2021650.

39 Rous P (1966) The Challenge to Man of the Neoplastic Cell. Nobel Lecture. https://www.nobelprize.org/prizes/medicine/1966/rous/lecture/

40 Samson AL, Knaupp AS, Kass I, Kleifeld O, Marijanovic EM, Hughes VA, Lupton CJ, Buckle AM, Bottomley SP, Medcalf RL. Oxidation of an exposed methionine instigates the aggregation of

 doi:10.20944/preprints202604.2181.v1

glyceraldehyde-3-phosphate dehydrogenase. J Biol Chem. 2014 Sep 26;289(39):26922-26936. doi: 10.1074/jbc.M114.570275. Epub 2014 Aug 1. PMID: 25086035; PMCID: PMC4175333.

41 Shi M, Hou J, Liang W, Li Q, Shao S, Ci S, Shu C, Zhao X, Zhao S, Huang M, Wu C, Hu Z, He L, Guo Z, Pan F (2023) GAPDH facilitates homologous recombination repair by stabilizing RAD51 in an HDAC1-dependent manner. EMBO Rep 24(8):e56437. doi: 10.15252/embr.202256437. Epub 2023 Jun 12. PMID: 37306047; PMCID: PMC10398663.

42 Siede W, et al. (1993) RAD9-dependent G1 arrest defines a second checkpoint for damaged DNA in the cell cycle of Saccharomyces cerevisiae. Proc Natl Acad Sci U S A 90(17):7985-9 PMID: 8367452

43 Soulier J and Lowndes NF (1999) The BRCT domain of the S. cerevisiae checkpoint protein Rad9 mediates a Rad9-Rad9 interaction after DNA damage. Curr Biol 9(10):551-4 PMID: 10339432

44 Sweeney FD, et al. (2005) Saccharomyces cerevisiae Rad9 acts as a Mec1 adaptor to allow Rad53 activation. Curr Biol 15(15):1364-75 PMID: 16085488

45 Thomas GE, Egan G, García-Prat L, Botham A, Voisin V, Patel PS, Hoff FW, Chin J, Nachmias B, Kaufmann KB, Khan DH, Hurren R, Wang X, Gronda M, MacLean N, O'Brien C, Singh RP, Jones CL, Harding SM, Raught B, Arruda A, Minden MD, Bader GD, Hakem R, Kornblau S, Dick JE, Schimmer AD. (2022) The metabolic enzyme hexokinase 2 localizes to the nucleus in AML and normal haematopoietic stem and progenitor cells to maintain stemness. Nat Cell Biol. 24(6):872-884. doi: 10.1038/s41556-022-00925-9. Epub 2022 Jun 6. PMID: 35668135; PMCID: PMC9203277.

46 Toh GW and Lowndes NF (2003) Role of the Saccharomyces cerevisiae Rad9 protein in sensing and responding to DNA damage. Biochem Soc Trans 31(Pt 1):242-6 PMID: 12546694.

47 uniprot/P60174 https://www.uniprot.org/uniprotkb/P60174/entry#disease_variants

48 Vander Heiden MG, Cantley LC, Thompson CB. Understanding the Warburg effect: the metabolic requirements of cell proliferation. Science. 2009 May 22;324(5930):1029-33. doi: 10.1126/science.1160809. PMID: 19460998; PMCID: PMC2849637.

49 Vialard JE, et al. (1998) The budding yeast Rad9 checkpoint protein is subjected to Mec1/Tel1-dependent hyperphosphorylation and interacts with Rad53 after DNA damage. EMBO J 17(19):5679-88 PMID: 9755168

50 Wang S, Ramamurthy D, Tan J, Liu J, Yip J, Chua A, Yu Z, Lim TK, Lin Q, Pines O, Lehming N. Post-translational Modifications of Fumarase Regulate its Enzyme Activity and Function in Respiration and the DNA Damage Response. J Mol Biol. 2020 Nov 20;432(23):6108-6126. doi: 10.1016/j.jmb.2020.09.021. Epub 2020 Oct 12. PMID: 33058874.

51 Wang J, Yu X, Cao X, Tan L, Jia B, Chen R, Li J. (2023) GAPDH: A common housekeeping gene with an oncogenic role in pan-cancer. Comput Struct Biotechnol J. 21:4056-4069. doi: 10.1016/j.csbj.2023.07.034. PMID: 37664172; PMCID: PMC10470192.

52 Weinberg RA (2014) The Biology of Cancer. 2nd Ed. Garland Science.

53 Weinert TA and Hartwell LH (1988) The RAD9 gene controls the cell cycle response to DNA damage in Saccharomyces cerevisiae. Science 241(4863):317-22 PMID: 3291120

54 Weinert T (1998) DNA damage checkpoints update: getting molecular. Curr Opin Genet Dev 8(2):185-93 PMID: 9610409

55 Weinert TA and Hartwell LH (1990) Characterization of RAD9 of Saccharomyces cerevisiae and evidence that its function acts posttranslationally in cell cycle arrest after DNA damage. Mol Cell Biol 10(12):6554-64 PMID: 2247073

 doi:10.20944/preprints202604.2181.v1

56 WHO, World Health Organisation (2023) Fact Sheet on Cancer: https://www.who.int/news-room/fact-sheets/detail/cancer

57 Yang W, Xia Y, Hawke D, Li X, Liang J, Xing D, Aldape K, Hunter T, Alfred Yung WK, Lu Z. PKM2 phosphorylates histone H3 and promotes gene transcription and tumorigenesis. Cell. 2012 Aug 17;150(4):685-96. doi: 10.1016/j.cell.2012.07.018. Erratum in: Cell. 2014 Aug 28;158(5):1210. PMID: 22901803; PMCID: PMC3431020.